5G-NR Network Planning: Impact of Massive MIMO and Beamforming in Coverage Predictions

Pedro Lopes Sousa*, António Rodrigues* and Helena Catarino†,
*Instituto Superior Técnico
†Nokia Portugal

***Abstract*—The fifth generation of mobile communications, 5G, aims to meet the growing needs and greater demand of users in relation to capacity and latency, in a growth that has been exponential and that is expected to continue. This thesis aims to analyse the impact of MIMO and beamforming antennas - whose technology is promising to meet the requirements - on the network's performance, through coverage predictions. This assessment was made using a radio network planning tool from Nokia Portugal, a partner in this thesis. Four studies were carried out, evaluating network coverage, quality and capacity: impact of active antennas on passive antennas in single user MIMO mode; performance comparison between active antennas in single user MIMO and multi-user MIMO mode; and lastly the impact of the different beam set configurations on the cell's capacity. The results provided by the active antennas shown to have a positive impact, confirming an increase of the cell capacity, of about 8 times, regarding the passive antenna. In single user mode, no significant differences were observed between the active antennas under study, contrary to what was observed in multi-user mode, in which the number of transceivers confirmed the increase in cell capacity. Finally, the capacity of the cell with antennas with vertical beamforming proved to be dependent on the gain of the beams, as users were not distributed over different heights.**

***Index Terms*—5G, beamforming, MaMIMO, coverage, capacity, AAS, beam set**

I. Introduction

The tremendous increase in the number and variety of connected devices, the significant increase in the volume and types of user/network traffic suchlike social media apps, gaming, streaming, as well as the performance constraints of Fourth Generation (4G) technologies, have motivated industry efforts and investments to define, develop and deploy the Fifth Generation (Fifth Generation (5G)) of mobile network. For the first time, in 2018, among the population covered by a mobile broadband network, there were more mobile internet users than non-users [1]. With the increasing of connected users each year, it is expected a continuous increasing throughout the following years. According to [2], audio and video streaming will become prevalent and the highest contributors to the increased traffic demand (about 79% of demand by 2020), while cloud storing services will see the most growth, which can be seen in figure 1.

5G can be considered a continued evolution of Long Term Evolution (LTE), since LTE is being optimised for more and more use cases until it eventually fulfills the International Mobile Telecommunications (IMT)-2020 requirements and a 5G technology can be labeled, which is not only a new or evolved Radio Access Technology (RAT), but a well integrated and seamlessly interoperable RATs. Furthermore, 5G is intended to allow a networked society where data can be accessed and shared by anyone and anything, anywhere and anytime. For this reason, three different types of service and consumer specifications are targeted: Enhanced Mobile Broadband (eMBB), Massive Machine Type Communication (mMTC), and Ultra-reliable Low Latency Communication (uRLLC). The first is driven by offering high data rates to support future multimedia services and the growing volume of traffic; the second by the Internet of Things (IoT) growth and the need for establishing connections between machine equipments, e.g., remote sensors, monitoring systems; and the last one by the very low latency and extremely high reliability of the machine-type communications. At this stage, based on the Third Generation Partnership Project (3GPP) release 15, 5G-New Radio (NR) network is focused on eMBB service, so the target of 5G-NR at this time is to meet the eMBB requirements. Hence, this present work is focused on promising wireless technologies such as Massive MIMO (MaMIMO) and beamforming, that are expected to meet the requirements for addressing high data rates to the end-user.

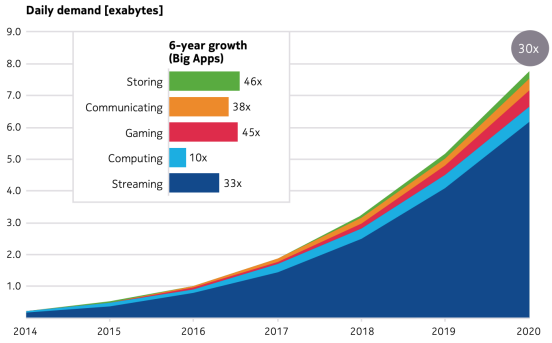

Fig. 1: Daily demand by category over the last 6 years [2].

This study is based on a radio network planning tool, in a collaboration with Nokia Portugal, part of the well known Finnish multinational telecommunications leader company.

II. 5G-NR Basic Concepts

5G will initially work with existing 4G networks before evolving into fully independent networks in subsequent releases and extensions of coverage. The possibility of operating a radio access technology in different frequency bands, where NR do not assume any specific band can make use of the

low frequencies (i.e., below 6 GHz) for coverage and high frequencies when high throughput and low latency operations are required (i.e., mmWave band). In terms of Modulation and Coding Scheme (MCS), NR supports Quadrature Phase Shift Keying (QPSK), 16 Quadrature Amplitude Modulation (QAM), 64 QAM and 256 QAM modulation formats for both uplink and downlink, as in LTE. Lower MCS (under 64-QAM) are more robust (i.e., least chance of losing data) and tolerant to higher values of interference although at a lower transmission throughput, while higher MCS orders (64-QAM and above) have much higher transmission throughput, but are less robust (i.e., greatest chance data can be lost) and more sensitive to noise and interference [3]. The extensive research on multiple access has shown that Orthogonal Frequency Division Multiple Access (OFDMA) is able to provide both downlink and uplink with fairly high system throughput for eMBB [4], hence being at least mandatory for NR. With the new range of frequencies required by 5G-NR, specially in the highest frequencies, propagations conditions are more challenging due to the very fast attenuation of the signal. Beamforming and Massive MIMO (MaMIMO) can be used as a tool to improve link budgets by providing higher number of data streams, focusing the radiation pattern of an antenna directly towards the specific user device, hence increasing the received signal strength and consequently the end-user throughput. Simultaneously to the work on the 3GPP NR radio-access technologies, the overall system architectures were reviewed, namely the Radio Access Network (RAN) and the Core Network (CN) and respective functionalities.

A. 5G-NR Network Architecture

5G network architecture aims to be flexible, virtualising the RAN, with network slicing, which is much more service oriented than previous generations.

For CN-RAN deployment, 3GPP has fixed several options.

The first rollout of 5G networks will be anchored by LTE (Non-standalone (NSA) deployments), allowing the mobile network operators to leverage their current networks, and still supply their costumers with high data speed connectivity. Taking this into account, 3GPP option 3, is a non-standalone option where radio access network is composed of a LTE base station (Evolved Radio NodeB (eNB)s) as the master node and 5G base sation (New Radio NodeB (gNB)s) as the secondary node. They are connected by the X2-interface. The radio access network is connected to Evolved Packet Core (EPC) by the legacy S1-interfaces. In this scenario, the NR gNB is seen by the EPC as a secondary RAT within LTE Radio Access Network (E-UTRAN). LTE is used as the control plane anchor for NR, and both LTE and NR are used for user data traffic (user plane). The NR gNB may have a user plane connection over S1 to Serving Gateway (SGW), but no control plane connection over S1 to Mobility Management Entity (MME), so the data routing will vary depending where to split the user plane between LTE and 5G [5]. Taking into account these variants, option 3 is divided into: option 3, option 3a, option 3x - illustrated in figure 2 and detailed below [6].

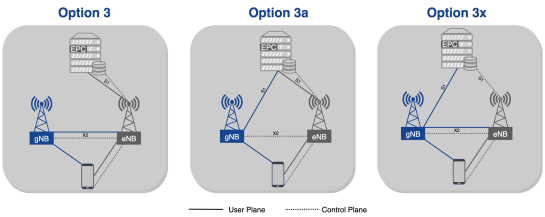

Fig. 2: CN-RAN deployment options.

Option 3 has the user data split in the LTE eNB. In this scenario, eNB nodes will carry a large amount of traffic and computer load, not being efficient. Option 3a has user data split in the EPC. This means no sharing of data load between the nodes. Option 3x is a combination between option 3 and 3a, having the data split in the 5G gNB. By using 4G as the anchor point of the control plane, the service enhancements provided by the 5G gNB and the small impact on the existing network, Option 3x has become the mainstream choice for NSA deployments [7][5]. A generic operation of this option is shown in figure 3. While downloading or streaming packets, if the User Equipment (UE) enters the gNB area, the bearer path once connected to the eNB is switched to the gNB and the device is served of additional user plane capacity. In case of an incoming voice call, the IP Multimedia Subsystem (IMS) architecture framework enables the delivery of multimedia services over any access network, for example Voice over New Radio (VoNR), and the voice packets run through a different bearer over the eNB, while the service is managed by the eNB.

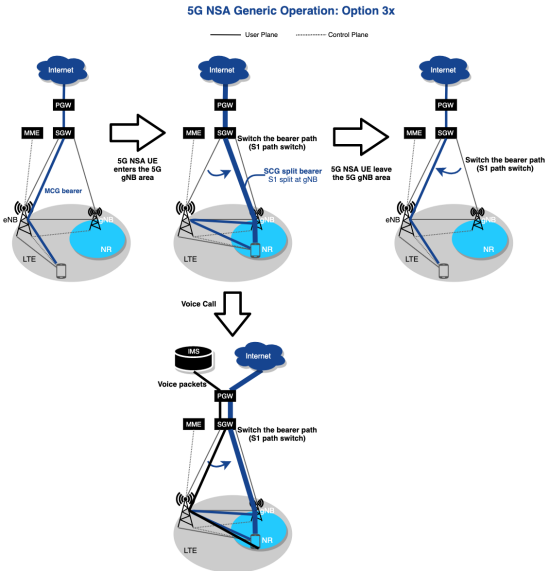

Fig. 3: 5G NSA option 3x - generic operation (adapted from [8]).

B. Physical Layer

The physical layer is the backbone of 5G-NR, as with any wireless technology, and is responsible for the step-by-step process of converting bits into radio waves. Channel coding

is one of the first processing steps, regarding protection and encryption of the information. Thereafter, modulation takes place, where bits are converted into modulation symbols. Modulation schemes supported are QPSK, 16 QAM, 64 QAM and 256 QAM, where each modulation symbol corresponds to 2, 4, 6 or 8 bits respectively. After mapping the modulated symbols onto parallel streams, they are multiplied by a different subcarrier frequency, equally spaced as they achieve orthogonality between subcarriers, defining a digital multi-carrier scheme called Orthogonal Frequency Division Multiplexing (OFDM). Finally the digital OFDM signal is converted to an analogue signal and up-converted to the selected carrier frequency (e.g., prime 3.5 GHz [9]).

There are three different types of channel in the radio channel architecture: logical channels, transport channels and physical channels. A distinction can be made between physical channel, on which they carry data and information from higher layers incl. control, scheduling and user payload; and physical signals, generated in Layer 1 (hence does not carry information originating from higher layers) and used for system synchronisation, cell identification and radio channel estimation [10].

Some of the synchronisation signals, particularly Primary Synchronisation Signal (PSS), Secondary Synchronisation Signal (SSS) and the Physical Broadcast Channel (PBCH) together form an Synchronisation Signal (SS)/PBCH block, also known as Synchronisation Signal Block (SSB), that is transmitted in four OFDM symbols across 240 subcarriers in the frequency domain and in predefined bursts across the time domain, whose periodicity in terms of time slots relies on which subcarrier spacing numerology is set. The PBCH carries the Master Information Block (MIB), and its own demodulation reference signal (DMRS). In case of beamforming, each beam transmits the same PSS and SSS, same MIB, excepting the demodulation reference signal (DMRS) that is different and allows the identification of each beam. All the SSB transmitted, regardless of number of beams, are arranged in periodical burst series within one half radio frame (5ms).

As the SSB is repeated for each beam during the sweeping, in respect to the UE, a search and measure is made for the beams, identifying which beam was received the best, and providing corresponding feedback for the gNB.

1) Transmission Scheme and Radio Frame Structure: In order to support a wide range of deployment scenarios, the NR supports flexibility in the OFDM numerology with a subcarrier spacing varying from 15 kHz to 240 kHz, and adjusting the numerology applied based on traffic patterns and other application parameters. Numerologies with wider subcarrier spacings are also optimal for low latency services since the duration of the transmission slot is inversely proportional to the subcarrier spacing. The 15 kHz numerology is identical to the one used in LTE, with a slight difference in the number of OFDM symbols per slot, as in LTE is 7 OFDM symbols whilst in NR is 14 OFDM symbols. The duration of radio frame and subframe are established as 10 ms and 1 ms, respectively. A Physical Resource Blocks (PRB) consists of 12 consecutive subcarriers in the frequency domain. A NR radio carrier is limited to 3300 active subcarriers (275 PRB) which results in carrier bandwidths of 50, 100 and 200 MHz for Subcarrier Spacing (SCS) of 15, 30/60 and 120 kHz, respectively [11].

2) Duplex Scheme: All 5G bands above 3 GHz will adopt Time Division Duplex (TDD) [12]. TDD has a major advantage in the use of a single frequency band where downlink and uplink occur in alternating time slots, thus being time-multiplexed. A guard time is provided without transmission to permit the switching between transmissions and, therefore, avoid interference. NR also makes use of dynamic TDD, where a slot can be dynamically allocated by the scheduler to either downlink or uplink transmission.

C. Multi-antenna Transmission

The reduction of the physical tower space, the integrated signal amplifiers, the ability to electronically tilt transmission beams and steer them [13], makes the Active Antenna Systems (AAS) a viable option for 5G networks. Depending on the number of users, mainly two types of multi-antenna systems can be deemed: Single User MIMO (SU-MIMO) and Multi-User MIMO (MU-MIMO). In single-user Multiple Input Multiple Output (MIMO) the information is transmitted simultaneously between different multiple data layers towards a target UE where each layer is separately beamformed thereby improving peak user throughput and system capacity [14], whereas in multi-user MIMO the difference is mostly the plural number of users, as the base station communicates with multiple devices using a separate stream for each. While SU-MIMO increases the data rate of just one user, MU-MIMO allows to increase the overall capacity as well as having better spectral efficiency (bit/s/Hz) than SU-MIMO [15].

1) Beamforming: is an enabling technique that directs the radiation pattern of an antenna towards a specific receiving device. Through adjusting the phase and amplitude of the transmitted signals, the overlapping waves will produce constructive (and destructive) addition of the corresponding signals, which can increase the received signal strength and therefore the end-user throughput [16]. The recent availability of new flexible antenna techniques, with vertical and horizontal antenna pattern adaptation, enables a fully dynamic adaptation and control of the antenna pattern in 3D. This feature associated with the MIMO capability of employing additional spatial diversity can impact positively the quality of the signal, the number of users served and consequently achieve better spectral efficiency.

All parameters related to the configuration of beams used in a cell are collected in a beam set. The core of such a beam set is the distribution of the SSB beams in the angular space which covers the cel, called basic beam set, which can be distributed and vary in rows and columns. There is a nomenclature used to distinguish the different configurations, where the number of columns in a row is given by the respective integer, preceded by the character '#'.

Each SSB beam has four refined beams implemented, that carry Channel State Information (CSI) and physical channels,

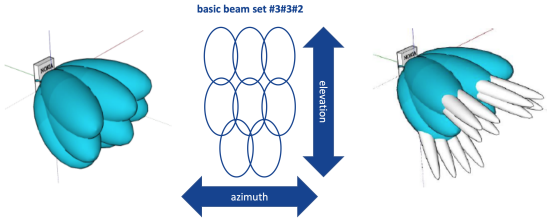

Fig. 4: Basic beam set #3#3#2.

and are used to achieve higher Carrier-to-interference-plus-noise Ratio (CINR) for a single UE, as well as to better separate multiple UEs in MU-MIMO operation.

2) Massive MIMO: refers to the large number of antennas in the base station antenna array (typically tens or even hundreds) and MIMO (Multiple-Input Multiple-Output) technology, as the name suggests, is a wireless technology that uses multiple transmitters and receivers to transfer more data at the same time, with which spatial multiplexing is achieved. The spectral efficiency grow just about linearly with the number of antennas of MaMIMO [17] and it is related with the Signal to Interference plus Noise Ratio (SINR) improvement due to narrower beams. The high degree of energy concentration in space from the narrower beams increases the signal strength provided to the UE location and less power is spreaded in other direction, causing lower level of interference. It is possible to fit a considerable amount of antenna elements in the array, as the inter-spacing between antenna elements should be in the order of the wavelength, at least half of the wavelength ($\lambda/2$), thus the antenna panels can have a very reduced size at high frequencies. Polarisation diversity also plays an important role, where one antenna radiating element consists of two ports that radiate orthogonal polarisations, reducing the transmit-array size by half compared to a spatially separate single-polarized transmit-array [18].

The capacity increases with the number of antenna ports [6], that is, increasing the number of independent data streams (layers) allows to send data to multiple UEs in parallel but, conversely, leads to an increase of the power consumption and costs. Furthermore, the number of antenna elements defines the antenna gain, which controls coverage, that is, more antenna elements results in more coverage.

In order to obtain the benefits of additional antennas and to fully enjoy the capacity gain offered by MaMIMO, it is needed to characterise the spatial channel between the antenna elements and the UE, generally referred as CSI TDD plays an important role by by using the reciprocity of the channel [19] (using the same frequency band) and therefore reduces the overhead of CSI. This spatial transfer functions and information are then collected and gathered in a matrix that is constantly being updated by the feedback of the users.

III. Simulator Description

The *9955 Radio Network Planning (RNP)* tool is a fine-tuned network planning software from *Forsk* company, perfectly adapted for Nokia networks.

This study is made by means of coverage predictions, where the signal levels are calculated in every pixel. The coverage of a mobile network is directly related to the range of the received signal in conditions that still allow the reception and decoding of the signal.

Before making predictions, it is necessary to create the network. The information related to the propagation model, sites, cells, and transmitters must be filled in, followed by the clutter and morphology classes information. The considerable amount of parameters that can be configured either for the site, transmitter or cell, elevates the high number of freedom degrees, opening a way to optimisation.

A. Propagation Model

The propagation models can be based on measurements and statistical adjustments, called empirical models, or based on physical laws and electromagnetic theory, called deterministic models. While the latter model requires a detailed information about the propagation environment, empirical models are simpler and require less computation effort.

For this thesis, the A9955 Standard Propagation Model (SPM) was adopted, with a 2.5D database. This type of database takes into account the terrain database and the clutter classes plus an additional layer of average heights per clutter class. The SPM is an empirical model and it was developed based on the Hata path loss formulas. This model is apt for the 150 - 3500 MHz frequency band, which evidently comprises the 3.5 GHz or n78 band defined by 3GPP. It determines the large-scale fading of received signal strength over a distance range of one to 20 km [20]. The Standard Propagation Model is based on the following formula [21], where each K is influenced by the type of terrain, diffractions, the height of both receiving and transmitting antennas, and the clutter classes:

$$\begin{aligned} P_R = P_{Tx} - \Big(& K_1 + K_2 \cdot \log(d) + K_3 \cdot \log(H_{Tx_{eff}}) + \\ & K_4 \cdot DiffractionLoss + K_5 \cdot \log(d) \cdot \log(H_{Tx_{eff}}) + \\ & K_6 \cdot H_{Rx_{eff}} + \\ & K_7 \cdot \log(H_{Rx_{eff}}) + K_{clutter} \cdot f(clutter) + K_{hill,LOS} \Big) \end{aligned} \tag{1}$$

where:

- P_R: received power [dBm]
- P_{Tx}: transmitted power [dBm]
- K_1: constant offset [dB]
- K_2: multiplying factor for log(d)
- d: distance between the transmitter and the receiver [m]
- K_3: multiplying factor for $\log(H_{Tx_{eff}})$
- $H_{Tx_{eff}}$: effective height of the transmitter antenna [m]
- K_4: positive multiplying factor for diffraction calculation ($K_4 \geq 0$)
- $DiffractionLoss$: losses due to diffraction over an obstructed path [dB]
- K_5: multiplying factor for $\log(d) \cdot \log(H_{Tx_{eff}})$

- K_6: multiplying factor for $H_{Rx_{eff}}$
- K_7: multiplying factor for $\log(H_{Rx_{eff}})$
- $H_{Rx_{eff}}$: mobile antenna height [m]
- $K_{clutter}$: multiplying factor for $f(clutter)$
- $f(clutter)$: average of weighted losses due to clutter
- $K_{hill,LOS}$: corrective factor for hilly regions ($= 0$ in case of NLoS)

All this parameters can be configurable by the user for specific studies yet most of the parameters are already pre-defined and calibrated based on extensive measurement campaigns and experiments in the biggest cities and capitals, which are taken by default by most of the vendors when planning radio networks. To a more realistic approach, the losses by clutter class were also taken into account and adjusted to the band used, following Nokia internal guidelines.

B. Network Configuration Parameters

Some parameters maintain the same configuration regardless of the prediction. The main resolution is set to 5 meters, and it determines the size of a pixel. This is the resolution of every geographic database and for every prediction. The antenna height is set to 30 meters, and the frequency band is n78, 3.5 GHz, which is the centre frequency of the carrier, with 100 MHz of bandwidth operating in TDD duplexing method. The diversity support covers SU-MIMO and MU-MIMO, and the traffic load is set to 100% in order to assess the predictions in full load capacity. The radio equipment selected (from gNB) operates below 6 GHz, with configured bearer selection thresholds, bearer efficiency, and MIMO gains. The site parameters are simply the geographical location of the base station and will be detailed ahead.

1) Transmitter Parameters: Once the site is configured, the transmitters can be inserted, which they can be modified from prediction to prediction. All the antennas have 90 degrees of azimuth (pointing east), with 0 degrees of mechanical downtilt and 4 degrees of additional electrical downtilt, which is function of the antenna's height. The number of transmission antennas, receptions antennas and power amplifiers is 16, 32 and 64 and will vary according to the antenna selected for study. The noise figure of every antenna is 3 dB.

2) Cell Parameters: The cell parameters allow to define the Radio Frequency (RF) channel on a transmitter. The cell's maximum power is 52 dBm, the minimum SS-Reference Signal Received Power (RSRP) required for a user to be connected to the cell is -121 dBm, the numerology is 1 - SCS (30 kHz). The scheduler operates in proportional fair, that is, allocates the same amount of resources to all the users with a maximum throughput demand. The number of users will be 1 or 10, depending on the study, and the beam usage that represents the repartition of each beam index in percentage is automatically calculated by the tool.

C. Deployment Area and Inputs

In this study it is chosen an urban area of approximately 6.3 km^2 located in Munich, Southern Germany, for the purpose of studying the impact of beamforming and MaMIMO antennas in an urban environment.

Fig. 5: Deployment area

In *9955 RNP*, the terrain database like Digital Terrain Model (DTM), as well as the ambient database like clutter classes and clutter heights are the inputs of geographic data used in the predictions. Each pixel in a clutter class file contains a code that corresponds to a clutter class, where each clutter class has an associated attenuation value.

D. Antennas

Two types of antennas are used in this study: a passive antennas and active antennas (featuring MIMO and 3D beamforming), in order to study the impact regarding these technologies. There is three active antennas under study: AAS16, AAS32 and AAS64. Each of them has the same number of antenna elements (192) and horizontal radiation width (90 degrees). They differ in the number of Transceiver (Tx) and Receiver (Rx) which is 16, 32 and 64; the number of data streams, which is 8 to the AAS16 and 16 to AAS32 and AAS64; and the basic beam sets, which they only have in common the #8. Every 3D beamforming antenna generates 40 beams, 8 control channel beams (used for SS/PBCH) and 32 traffic channel beams (used for Physical Downlink Control Channel (PDCCH), Physical Downlink Shared Channel (PDSCH), etc.). The beam gains will vary according to the beam set configured, between 19.7 and 23.6 dBi. In the other hand, the passive antenna is a traditional 2x2 MIMO antenna, with two column passive antenna and two radios, with polarisation diversity. It will be operating under the same conditions, that is, same frequency band (3.5 GHz), bandwidth of 100 MHz, same maximum power (52 dBm), same horizontal radiation width (90^o), except the antenna gain that is equal to 14.5 dBi.

E. Traffic Parameters

Every coverage prediction has associated several parameters regarding the traffic, namely the user's profile, the type of service, the user's mobility and the terminal used by the user. The service targeted for 5G NR deployment is broadband, the lowest modulation is QPSK and the highest is 256QAM. The coding rate ranges from 0.1 to 0.99. The user terminal operates below 6 GHz, with minimum power of -40 dBm and 23 dBm maximum. The noise figure is 8 dB, and the number of Tx/Rx is 1 and 4, respectively. The receiver's (user) height is set to 1.5 meters.

F. Predictions

In order to assess the signal levels and signal quality, four types of coverage predictions are available:

- **Network Coverage**: Predicts the effective signal levels of different types of 5G NR signals in the study area, and is represented by the SS-RSRP prediction.
- **Network Quality**: Predicts the interference levels and signal-to-interference levels in the study area and is represented by the PDSCH CINR levels.
- **Service Areas**: Calculates and displays the 5G NR radio bearers based on CINR for each pixel. This prediction is represented by the modulation schemes.
- **Network Capacity**: Calculates and displays the channel throughputs and cell capacities based on CINR and bearer calculations for each pixel. The assessment will be made by the effective Radio Link Control (RLC) throughput measure.

In *9955 RNP*, there is 2 different types of gains applied to SU-MIMO and MU-MIMO configurations: diversity gain and capacity gain. The diversity gain is applied to the CINR level and takes into account the number of transmission and reception antennas applied on the signal, improving the CINR, whereas the capacity gain is applied to the throughput and takes not only the number of antennas into account but also the number of MIMO users that share the same resources. In MU-MIMO, schedulers are able to allocate resources over spatially multiplexed parallel frames in the same frequency-time resource allocation plane. The proportional fair scheduler chosen can apply an extra gain, increasing the average cell throughput, called multi-user diversity gain, that depends on the number of simultaneously connected users to the cell.

IV. Results

In order to assess the impact of Massive MIMO and beamforming, four different analysis are made, evaluating the network coverage, quality and capacity. A comparison is made between the passive antenna and an active antenna (AAS16), in SU-MIMO, followed by the comparison, also in SU-MIMO, between every AAS. Furthermore, it is compared the AAS performance, but in MU-MIMO, and lastly a comparison of the results given by the different beam set configurations. Each pixel is considered a non-interfering user, with the traffic parameters assigned previously.

A. Passive Antenna vs Active Antenna

An active antenna, AAS16, and the passive antenna are compared in order to evaluate how Massive MIMO and beamforming affects the performance of the network coverage, capacity and quality, in SU-MIMO.

1) Network Coverage: The active antenna AAS16 covered 16% more area than the passive antenna. The AAS16 not only covered more area, but also with a stronger signal level - as shown in figure 6 - with average values of -109.11 dBm and -103.92 dBm for the passive and active antenna, respectively. This is mostly related to the fact that there's a difference of 9.1 dBi in the antenna gain, which is responsible for providing

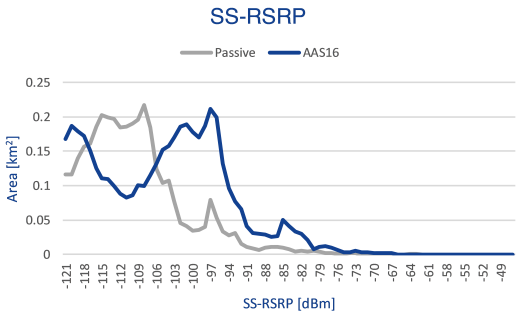

Fig. 6: Frequency polygon of the SS-RSRP level by covered area.

a greater received signal power in pixels near the transmitter and exceed the minimum threshold to be connected to the cell in farther pixels, by the greater coverage distance achieved by the beams. The antenna gain is influenced by the number of antenna elements, whose number in the active antenna exceeds the passive one. Despite the difference in the antennas, both antennas demonstrated similar coverages, knowing that MaMIMO and beamforming are more driven by capacity than coverage.

2) Network Quality: Since only one cell was deployed, no interference from other cells is expected, thus the prediction is only dependent on the PDSCH signal level and the noise, which is constant. The active antenna AAS16 achieved better CINR values - which can be seen in figure 7 - with an average PDSCH CINR value of 0.98 dB and 15.98 dB for the passive and active antenna AAS1, respectively. This result is due to a diversity gain regarding the number of transmission antennas. On account of the CINR values, different radio bearers thresholds are triggered, providing better bearer efficiency and coding rates to the transmission.

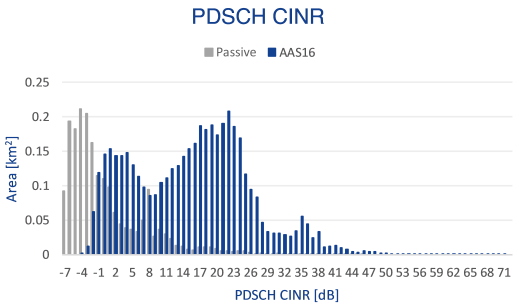

Fig. 7: PDSCH CINR histogram by covered area.

The modulation schemes, shown in figure 8, are fully dependent on the radio bearers. Therefore a high percentage of QPSK is expected for the passive antenna, in contrast with active antenna that expects a much higher percentage in the best modulations, which is confirmed.

3) Network Capacity: The aim of the network capacity coverage prediction is to assess the amount of data traffic that

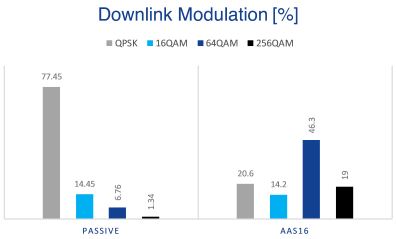

Fig. 8: Modulation schemes of the coverage prediction.

a network can provide in a given area. This measurement is based on the CINR and radio bearer calculations for each pixel, determining the highest bearer at each pixel and multiplying the bearer efficiency (bits/symbol) by the number of symbols in the Downlink (DL) frame to determine the RLC layer throughputs. The differences are shown in figure 9, with a calculated mean value of 40.370 Mbps in the passive antenna, in contrast with the 328.179 Mbps of the active antenna, an improvement of more than 8 times the throughput mean value, mostly due to the fact that the AAS can transmit more parallel data streams than the passive antenna, and in more pixels, increasing the cell throughput and spectral efficiency.

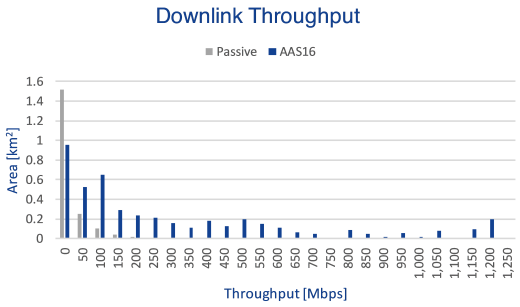

Fig. 9: Cell capacity histogram by covered area.

B. Comparison of AAS performance in SU-MIMO

In SU-MIMO (also called spatial multiplexing), the information is transmitted simultaneously over more than one data stream (or layer) using the same frequency/time resources to a single user. The three active antennas, AAS16, AAS32 and AAS64 are evaluated.

1) Network Coverage: The graph in the figure 10 represents a Cumulative Distribution Function (CDF), where the SS-RSRP resulting values are combined with respect to the area and shown along a curve.

Despite the difference in the number of Tx, the coverage is mostly influenced by the number of antenna elements (which is the same) and the antenna gain (which is the same). It is expected the same results, however the results of covered area are 72.9% for AAS16, 79.3% for AAS32 and 75.4% for AAS64. The small differences are mostly related with device-specific parameters, such as SSS-Energy per Resource Element (EPRE).

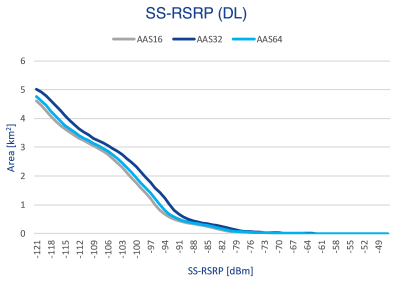

Fig. 10: SS-RSRP CDF by covered area.

2) Network Quality: The network quality is expected to achieve the same results for every AAS, since the number of streams of the MIMO system is limited by the number of transmitting or receiving antennas, whichever is lower, so is limited by the 4 Rx of the UE, regardless of the number of Tx. Despite that, the results diverge a bit - which can be seen in figure 11 - again due to device-specific parameters, suchlike physical channel power and EPRE. Analysing the mean value, the AAS32 attained 17.63 dB, 10.3% and 7.3% more in respect to AAS16 and AAS64.

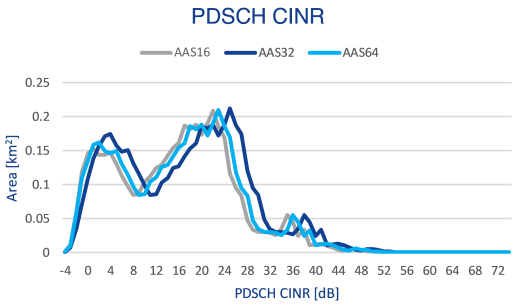

Fig. 11: Frequency polygon of the PDSCH CINR level by covered area.

The values reached by the CINR have direct repercussions on the modulation schemes, since the distribution is based on the CINR levels achieved in each pixel, which is confirmed in figure 12. The differences are mostly notable in higher modulations (64QAM and 256QAM).

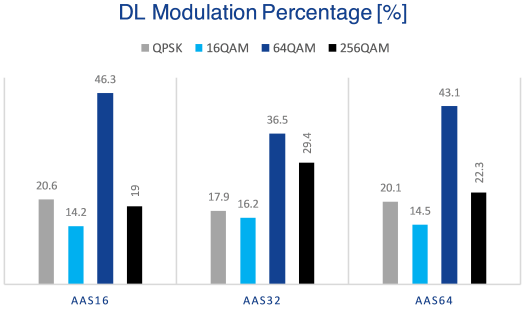

Fig. 12: Modulation schemes of the coverage prediction.

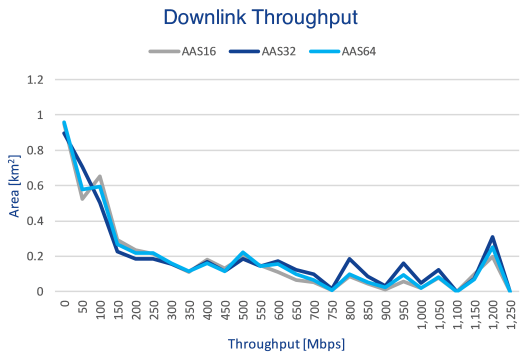

Fig. 13: Frequency polygon of the cell capacity by covered area.

3) Network Capacity: The use of spatial multiplexing with M transmission and N reception antenna ports can increase theoretically the throughput by M or N times, whichever is smaller. The UE only has 4 reception antenna ports, which means no capacity gain and improvement will be achieved regardless of the number of transmission antennas, because only 4 data streams will be received. This justifies the similar results obtained by every AAS, although the throughput performance of the AAS32 is slightly better, especially for throughputs above 550 Mbps - which can be seen in figure 13 - due to the also better CINR levels achieved previously. In this SU-MIMO case, the user throughput is equal to the cell throughput for the reason that all the resources are allocated towards one user.

C. Comparison of AAS performance in MU-MIMO

In MU-MIMO, data streams are distributed across multiple users on the same time/frequency resources, thus increasing the system capacity. In this study, 10 users were co-scheduled in proportional fair mode, i.e., allocation of the same amount of resources to all the users with a maximum throughput demand. The objective is to assess the impact of the diversity in the transmission antennas of AAS in MU-MIMO.

1) Network Coverage: It is observed the same SS-RSRP values as in SU-MIMO. Although the number of Tx stands different for every AAS, the coverage is primarily influenced by the number of antenna elements and consequently by the antenna gain. These characteristics have remained the same, hence the same coverage area was obtained. The number of users does not influence the coverage, since the reference signal is calculated in every pixel, independently if the pixel represents one user or multiple users.

2) Network Quality: The various data streams that each AAS can provide, can be used to serve different users simultaneously over the same time slot and frequency band. By accessing the channel state information, it is possible to encode the signals constructively by manipulating amplitudes and phases in the desired directions. This way it is possible to mitigate interference between the users connected in the cell, increasing the CINR. Since in this type of predictions there is no spatial distribution between the co-scheduled users, the radio planning tool applies a capacity gain in MU-MIMO configurations - which can be seen in figure 14 - increasing the mean value in the same covered area, of the AAS16, AAS32 and AAS64 to 16.86 dB, 18.02 dB and 18.43 db, respectively. This increase will result in radio bearers with higher efficiency and coding rates, so the modulation percentages are expected to be higher in the best modulations, which is confirmed in the figure 15.

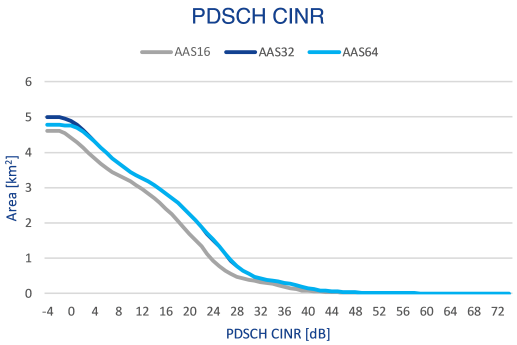

Fig. 14: PDSCH CINR CDF by covered area.

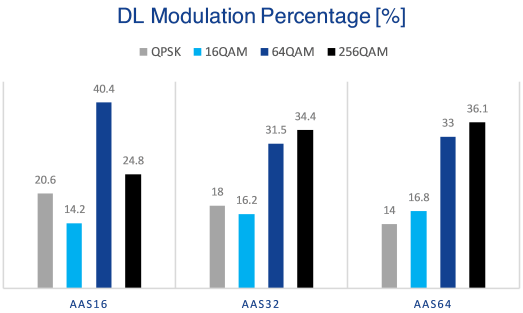

Fig. 15: Modulation schemes of the coverage prediction.

3) Network Capacity: The figure 16 represents the CDF of the cell capacity, which can be seen that the AAS16 and AAS32 achieve a maximum of approximately 2.4 Gbps, while the AAS64 can achieve cell throughputs of 4.4 Gbps, which represent 83% more than the first two.

It is clear that a capacity and multi-user gain was applied in every AAS by the *9955 RNP*. These gains vary according to the number of users connected to the cell, the Tx/Rx pair set and the almost 30 radio bearers that can be selected, thereby the gains aren't constant. In reality, independently of the gains applied by the network planning tool, it is expected that the increase in the number of transceivers results into an increase in cell capacity, due to the increase of independent data streams that are able to serve a greater number of users simultaneously, in the same bandwidth, thereby, increasing the spectral efficiency (bits/s/Hz).

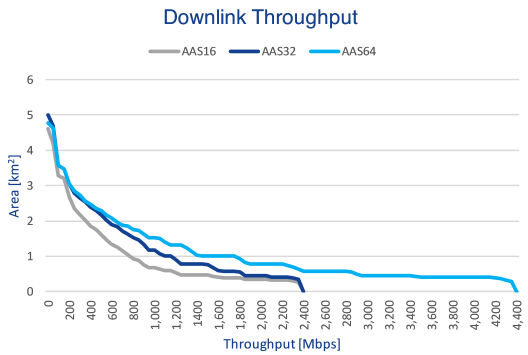

Fig. 16: Cell capacity CDF by covered area.

D. Impact of Different Beam Set Configurations

The later study identified the AAS64 antenna as the most advantageous, in terms of cell capacity and spectral efficiency. In order to assess the impact of different beam set configurations, this same antenna was selected for this study, with the following beam set configurations: #8, #6#2, #5#3, #4#4, #3#3#2 and #2#2#2#2. Every beam set configuration supports vertical beamforming, except the #8, which represent 8 beams in each column, in other words, 8 independent beams in the horizontal domain and a single vertical beam, merely allowing full exploitation of the horizontal beamforming. The #8 only applies vertical beam steering up to 6^{o} of range, whereas the remain has vertical beams, that allows to point vertically the main beam in the right direction where user scheduled is. These beam set have distinct beam gains by default, a device-specific configuration associated with the different distribution of the SSB beams, and are presented in the table below:

TABLE I: Beam set beam gains.

	#2#2#2#2	#3#3#2	#4#4	#5#3	#6#2	#8
Beam gain [dBi]	19.7	21.7	22.48	22.9	23.22	23.6

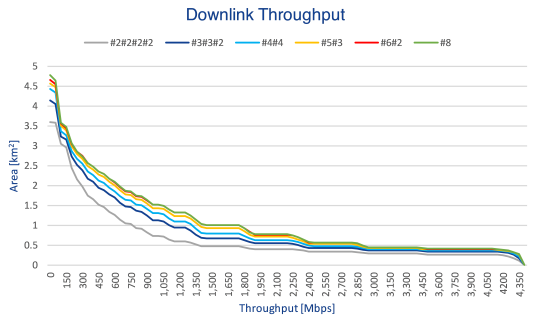

Fig. 17: Cell capacity CDF by covered area.

The beam gain associated has already been proven to be a parameter with direct consequences regarding coverage. In this study was no exception, as the beam set #8, with the highest beam gain, covered a greater percentage of area equal to 75.4% (18.7% more than the antenna with lower beam gain and 1.8% more than the second greater covered area). The highest DL throughput mean value is from the #6#2 beam set, with 1014.3 Mbps, 1.87% more than the second best, #8. However, it has less covered area. Looking closely to the graph in figure 17, it can be seen that its curve is mostly overlapped with the #8 beam set curve, except in the first 150 Mbps, whose coverage area of the beam set #8 is greater, thus lowering the mean value of the DL cell throughput, which can lead to an erroneous conclusion. Since both beam gains are very close, so as their results, none of them stand out. An extra prediction was made, setting the receivers height to 40m, instead of the usual 1.5m. As there is less obstruction in the line of sight, the throughput averages rose approximately 160%, however, always in agreement with the gain of the beams. In other words, the beam set with the highest beam gain (#8) obtained the best results, due to the beam steering. In short, if users are not distributed vertically at different heights, the gain of the beams is the most decisive factor for achieving better results, regardless of whether the antenna has more vertical beams. As they are all at the same height, there will be no additional gain in capacity from vertical beamforming, which can not only dedicate different beams simultaneously to different users in height, but also to reduce interference levels, thereby increasing spectral efficiency and the capacity of the cell, where it can have a big impact in scenarios of dense urban with high rise buildings.

V. Conclusion

The predictions showed the impact of MaMIMO and beamforming in active antennas when comparing to a traditional passive antenna, about 8 times more of cell capacity, while the difference in coverage is not that sharp, even knowing that MaMIMO and beamforming are more driven by capacity than coverage.

The performance of the active antennas in SU-MIMO is characterised by a link capacity, between the transmitter and the UE, which is limited by the number of receivers. Therefore, the results are expected to be similar, differentiated by device-specific parameters, which is confirmed.

On the other hand, MU-MIMO is characterised in terms of a system capacity, that is, the set of rates attainable for all UEs at the same time. It is expected that the increase in the number of transmission antenna ports, theoretically, lead to an increase of cell capacity and spectral efficiency, due to the increase of independent data streams that are able to serve a greater number of users simultaneously. This fact is confirmed and shows to be the key to unlocking higher spectral efficiencies.

Regarding the beam set configuration, it is expected an additional capacity gain due to the vertical beamforming, however, it wasn't confirmed since the users are not distributed vertically at different heights. The beams are steered instead, to the user location, hence making the beam gains the most decisive factor in the results achieved.

The predictions were based on a radio network planning tool, that besides being calibrated and tuned with Nokia

networks, are calculated by pixel and depend on a wide range of factors, thus can lack of accuracy comparing to reality.

REFERENCES

[1] GSMA, "The State of Mobile Internet Connectivity," 2019, last accessed June 2020. [Online]. Available: https://www.gsma.com/mobilefordevelopment/resources/the-state-of-mobile-internet-connectivity-report-2019/

[2] Nokia Bell Labs, "Who will satisfy the desire to consume?" last accessed June 2020. [Online]. Available: http://www.iot.gen.tr/wp-content/uploads/2017/03/160531-Nokia_Bell_Labs_Mobility_Traffic_Report.pdf

[3] A. Fragoso, "Impact of Massive MIMO Antennas on High Capacity 5G-NR Networks," Master's thesis, Instituto Superior Técnico, 2019.

[4] Y. Yuan and X. Wang, "5G New Radio: Physical Layer Overview," *ZTE Communications*, vol. 1, 2017.

[5] 3GPP, "Study on new radio access technology: Radio access architecture and interfaces," 3rd Generation Partnership Project (3GPP), Technical Specification (TS) 38.801, 3 2017, version 14.0.0. [Online]. Available: https://www.3gpp.org/ftp/Specs/archive/38_series/38.801/

[6] H. Holma, A. Toskala, and T. Nakamura, *5G Technology: 3GPP New Radio*. Wiley, 2020.

[7] GSMA, "5G Implementation Guide," July 2019, last accessed June 2020. [Online]. Available: https://www.gsma.com/futurenetworks/wp-content/uploads/2019/03/5G-Implementation-Guideline-v2.0-July-2019.pdf

[8] Harrison J Son, last accessed April 2020. [Online]. Available: https://www.netmanias.com/en/post/oneshot/14488/5g/5g-nsa-option-3a-3x-generic-operation

[9] Huawei Technologies Co. Ltd., "5G Spectrum - Public Policy Position." [Online]. Available: https://www-file.huawei.com/-/media/CORPORATE/PDF/public-policy/public_policy_position_5g_spectrum.pdf

[10] N. Chilamkurti, S. Zeadally, and H. Chaouchi, *Next-Generation Wireless Technologies: 4G and Beyond*, ser. Computer Communications and Networks. Springer London.

[11] R. Rios, "5G Network Planning and Optimization using Atoll," Master's thesis, Escola Tècnica d'Enginyeria de Telecomunicació de Barcelona, 2019.

[12] GSMA, "5G Spectrum - Public Policy Position," March 2020, last accessed June 2020. [Online]. Available: https://www.gsma.com/spectrum/wp-content/uploads/2020/03/5G-Spectrum-Positions.pdf

[13] D. Anzaldo, "LTE-Advanced Release-12 shapes new eNodeB transmitter Architecture: Part 1, Technology Evolution." [Online]. Available: https://www.maximintegrated.com/en/design/technical-documents/app-notes/6/6062.html

[14] 5G Americas, "Advanced antenna systems for 5G networks," Tech. Rep., 2019, last accessed June 2020. [Online]. Available: https://www.5gamericas.org/wp-content/uploads/2019/08/5G-Americas_Advanced-Antenna-Systems-for-5G-White-Paper.pdf

[15] L. Liu, R. Chen, S. Geirhofer, K. Sayana, Z. Shi, and Y. Zhou, "Downlink MIMO in LTE-advanced: SU-MIMO vs. MU-MIMO," *IEEE Communications Magazine*, vol. 50, no. 2, pp. 140–147, February 2012.

[16] Ericsson, "Advanced antenna systems for 5G networks," Tech. Rep., 2019, last accessed June 2020. [Online]. Available: https://www.ericsson.com/4a8a87/assets/local/reports-papers/white-papers/10201407_wp_advanced_antenna_system_nov18_181115.pdf

[17] C. Shepard, H. Yu, N. Anand, E. Li, T. Marzetta, R. Yang, and L. Zhong, "Argos: practical many-antenna base stations," August 2012.

[18] J.-K. Hong, "Performance Analysis of Dual-Polarized Massive MIMO System with Human-Care IoT Devices for Cellular Networks," *J. Sensors*, vol. 2018, pp. 3 604 520:1–3 604 520:8, 2018.

[19] J. Flordelis, F. Rusek, F. Tufvesson, E. G. Larsson, and O. Edfors, "Massive MIMO Performance-TDD Versus FDD: What Do Measurements Say?" *IEEE Transactions on Wireless Communications*, vol. 17, no. 4, pp. 2247–2261, April 2018.

[20] S. Popoola, P. A. Atayero, N. Faruk, C. Calafate, O. Abiodun, and V. Matthews, "Standard Propagation Model Tuning for Path Loss Predictions in Built-Up Environments," 07 2017, pp. 363–375.

[21] Nokia, "9955 RNP V7.4.0 Technical Reference Guide for Radio Networks," 2019, internal documentation.